Dalton Transactions

Accepted Manuscript

ROYAL SOCIETY OF CHEMISTRY

www.rsc.org/dalton

The effect of Li^+ ion on the luminescent properties of a single-phase white-light emitting phosphor α-$Sr_2P_2O_7$:Dy^{3+}

Bing Han[1]*, Pengju Li[1], Jingtao Zhang[2], Jie Zhang[1], Yongfei Xue[1], Hengzhen Shi[1]*

[1]School of Material and Chemical Engineering, Zhengzhou University of Light Industry, Zhengzhou 450002, People's Republic of China

[2]School of Food and Bioengineering, Zhengzhou University of Light Industry, Zhengzhou 450002, People's Republic of China

To whom correspondence should be addressed

Tel: 86-371-86609676

Fax: 86-371-86609676

E-mail: hanbing@zzuli.edu.cn (Bing Han),

shihz@zzuli.edu.cn (Hengzhen Shi)

Abstract

Two series of phosphors α-$Sr_{2(1-x)}Dy_{2x}P_2O_7$ and α-$Sr_{2(1-2x)}Dy_{2x}Li_{2x}P_2O_7$ with different x values were synthesized successfully by using a conventional solid state method at high temperature for the first time, and their luminescence properties were investigated comparatively. The effect of Li^+ ion on the luminescence properties of Dy^{3+} in α-$Sr_2P_2O_7$ host including luminescence intensity, optimal doping concentration, concentration quenching mechanism, decay behavior, and etc was discussed in detail by considering the defect generation in α-$Sr_2P_2O_7$:Dy^{3+}, the charge compensation of Li^+ ion and the role of Li_2CO_3 as solid flux expected in phosphors. The obtained excitation and emission spectra indicate these as-prepared phosphors can be excited by ultraviolet, and show white light emission due to the combination of the $^4F_{9/2}\rightarrow{}^6H_{15/2}$ and $^4F_{9/2}\rightarrow{}^6H_{13/2}$ transitions of Dy^{3+} ion. The CIE chromaticity coordinates and color correlated temperature of Dy^{3+} emission in the phosphor α-$Sr_{2(1-2x)}Dy_{2x}Li_{2x}P_2O_7$ (x = 0.03) with the optimal fluorescence intensity was also calculated. The present work could be helpful to understand the effect of the charge compensator (e.g. Li^+ ion) on the luminescent properties of phosphors with non-equivalent ion-displacement and design novel phosphors by efficiently taking advantage of charge compensator (e.g. Li^+ ion).

1. Introduction

Over the past few years, the topic that how to produce white light in a single-phase host has been the subject of much speculation by more and more research groups because of the advantages of high color rendering index (CRI), tunable correlated color temperature (CCT), pure Commission International de I'Eclairage (CIE) chromaticity coordinates, and averting the re-absorption existing in red–green–blue (RGB) tricolor phosphors for application in white-light emitting diodes (w-LEDs) [1]. White light generation in a single-phase host can be realized by four main methods: (1) doping singly a rare earth ion; (2) the combination of multiple rare earth ions; (3) co-doping ion pairs based on the energy transfer process; (4) defect-induced white light, which have been summarized by M. M. Shang et al. in their review paper in 2014 [1]. Compared with other methods, doping singly a rare earth ion is still the simplest and most straightforward method to obtain white light in a single-phase host material despite the luminous efficiency and intensity could be low. Among rare earth ions, Dy^{3+} ion can be most easily to realize white light emitting by the combination of its $^4F_{9/2} \rightarrow {}^6H_{15/2}$ (~480 nm, blue light) and $^4F_{9/2} \rightarrow {}^6H_{13/2}$ (575 nm, yellow light) transitions. Different from the white light from Eu^{2+} ion or Eu^{3+} ion, white light generation from Dy^{3+} ion is not influenced significantly by the crystal structure and the phonon frequency of the host lattice. As a well-known case, $YVO_4:Dy^{3+}$ phosphor has been applied commercially in high-pressure mercury lamps due to its efficient white-light-emitting [2]. Based on the significance of Dy^{3+} ion with white light emitting, many researchers have showed keen and persistent interest on the

luminescence properties of Dy^{3+} in inorganic phosphors and developed some novel and promising white-light-emitting phosphors with potential application prospect in display and lighting regions [3−10]. In addition, the hypersensitive $^4F_{9/2}\rightarrow{}^6H_{13/2}$ electric dipole transition of Dy^{3+} ion is sensitive to the chemical environment surrounding Dy^{3+} ion, so the yellow-to-blue (Y/B) emission intensity ratio ($^4F_{9/2}\rightarrow{}^6H_{13/2}$)/($^4F_{9/2}\rightarrow{}^6H_{15/2}$) also reflects the coordination surroundings of Dy^{3+} ion to some extent, so Dy^{3+} ions can be useful to probe the site symmetry of Dy^{3+} ion in a definite host lattice [4,9]. Thus, the investigation on Dy^{3+}-doped phosphors is still well worthwhile not only for potential industrial applications but also for basic research.

Phosphates are a large family of compounds including orthophosphates, pyrophosphates, metaphosphates, polyphosphates, and so on, which have been utilized as host materials of phosphors due to their relatively low material cost, easy synthesis, good thermal stabilities, and low sintering temperature [10,11]. $LaPO_4:Ce^{3+},Tb^{3+}$, as a famous green light emitting phosphor, has been applied in lamp industry for many years. A kind of alkaline earth pyrophosphate, α-$Sr_2P_2O_7$, is an important host material for luminescence of rare-earth metal ions and transition metal ions. Many research groups have paid lots of attention to the luminescence properties of α-$Sr_2P_2O_7$ based phosphors for potential application in display and lighting regions [11−20]. The related published papers were grouped mainly on three categories in term of the research contents. (1) Spectroscopic properties of α-$Sr_2P_2O_7$ doped with a single activator, e.g. α-$Sr_2P_2O_7:Ce^{3+}$, α-$Sr_2P_2O_7:U^{6+}$, α-$Sr_2P_2O_7:Bi^{2+}$ and etc [12−14].

(2) Energy transfer process among different activators in α-$Sr_2P_2O_7$ host, e.g. Sn^{2+}→Mn^{2+}, Eu^{2+}→Mn^{2+}, Ce^{3+}→Mn^{2+}, Ce^{3+}→Tb^{3+}, , Gd^{3+}→Eu^{3+} and etc [11,15−18].

(3) Long persistence phosphors based α-$Sr_2P_2O_7$, e.g. α-$Sr_2P_2O_7$:Eu^{2+},Y^{3+}, α-$Sr_2P_2O_7$:Eu^{2+},R^{3+} (R = Y, La, Ce, Gd, Tb and Lu), and etc [19,20]. As far as we known, though the high temperature combustion synthesis and thermoluminescence dosimetry application of Dy^{3+} activated α-$Sr_2P_2O_7$ was reported by N. Patel et al. in 2014 [21], the spectroscopic properties of α-$Sr_2P_2O_7$ doped with Dy^{3+} ions have not been investigated, and the related published work has not been found elsewhere. Li^+ ion, as a kind of charge compensator, often shows efficient luminescent enhancement for phosphors, in which the divalent alkaline earth ions were replaced by trivalent rare earth ions [22,23]. Meanwhile, Li^+ ion is often the optimal charge compensator among alkali metal ions such as Li^+, Na^+, K^+, Cs^+ for enhancing fluorescence intensity of phosphors. The reason can be Li^+ ion, with smaller radius, can be much easier to be incorporated into the host lattice [24−26]. Furthermore, Li^+ ion containing phosphor can have desirable fluorescence intensity. A typical example, $LiGd(PO_4)_3$:Eu^{3+} [27], has been considered to be a potential red phosphor for mercury-free lamps and plasma display panels (PDPs) in view of its emission intensity evaluated about 158% of commercial phosphor (Y,Gd)BO_3:Eu^{3+} under 172 nm excitation, in which the reason is unknown.

In view of the absence of luminescence investigation on Dy^{3+} ion in α-$Sr_2P_2O_7$ host, the possible effect of Li^+ ion on luminescence properties of phosphors, and possible direct white light generation from Dy^{3+} ions, in present work, we designed and

synthesized two series of phosphors α-$Sr_{2(1-x)}Dy_{2x}P_2O_7$ and α-$Sr_{2(1-2x)}Dy_{2x}Li_{2x}P_2O_7$ with different x values, and investigated comparatively their luminescence properties, focusing on the effect of Li^+ ion on luminescence properties of α-$Sr_2P_2O_7$:Dy^{3+} including luminescence intensity, optimal doping concentration, concentration quenching mechanism, decay behavior, and etc. The present work could not only enlarge the scope of research on luminescence properties of α-$Sr_2P_2O_7$ based phosphor, but provided some ideas on the development of novel phosphors with non-equivalent ion-displacement by efficiently taking advantage of charge compensator (e.g. Li^+ ion).

2. Experimental

Two series of polycrystalline powder samples with nominal chemical formula α-$Sr_{2(1-x)}Dy_{2x}P_2O_7$ (x = 0.001, 0.002, 0.003, 0.005, 0.01, 0.02, 0.03, 0.05) and α-$Sr_{2(1-2x)}Dy_{2x}Li_{2x}P_2O_7$ (x = 0.003, 0.005, 0.01, 0.02, 0.03, 0.05, 0.1) as well as the host compound α-$Sr_2P_2O_7$ were synthesized by a traditional high-temperature solid-state method. The reactants were $SrCO_3$ [analytical reagent (A.R.)], $NH_4H_2PO_4$ (A.R.), Li_2CO_3 (A.R.) and Dy_2O_3 (99.99 %), and used without further purification. The raw materials were carefully weighed stoichiometrically and ground in an agate mortar for at least 10 minutes until the mixture appeared homogeneous. Then the mixture was preheated at 673 K for 4 h in a muffle furnace, reground, and finally fired at 1173 K for 8 h in air with the heating rate of 3 K/min. The final products were cooled to room temperature (RT) by switching off the muffle furnace and crushed to fine particles for the next characterization.

The phase purity of the final products was characterized by a powder X-ray

diffraction (XRD) analysis with Cu K_α (λ = 1.5405 Å) radiation on a Bruker D8 Advance X-Ray Diffractometer. The morphology and size distribution of the sintered particles were observed with a scanning electron microscope (SEM, JSM-6490LV) and laser scattering particle analyzer (MICROTRAC S3500), respectively. Photoluminescence (PL) and photoluminescence excitation (PLE) spectra as well as decay curves were measured on a fluorescence spectrometer (HITACHI F-7000) equipped with a 150 W xenon lamp as the excitation source. Before the measurements of fluorescence spectra, each sample has been finely powdered under the same condition. Then, the sample was filled and pressed homogeneously between quartz windows in the Sample Well to keep the same measurement condition. All the measurements were performed at room temperature (RT).

3. Results and discussion

The XRD patterns for all as-prepared samples were characterized at RT, and as examples seven diffractograms for the samples with x = 0.001, 0.005, 0.05 for α-$Sr_{2(1-x)}Dy_{2x}P_2O_7$ and x = 0.003, 0.03, 0.1 for α-$Sr_{2(1-2x)}Dy_{2x}Li_{2x}P_2O_7$ as well as the α-$Sr_2P_2O_7$ host are shown in Fig. 1. The diffraction peaks for all the samples are similar to each other and all agree well with the Joint Committee for Powder Diffraction Standard (JCPDS) file 24-1011 (α-$Sr_2P_2O_7$), which indicates that all samples are of single pure phase. The substitution of Sr^{2+} by Dy^{3+} or Dy^{3+}/Li^{+} does not significantly influence the crystal structure. The host compound α-$Sr_2P_2O_7$ crystallizes in orthorhombic structure with space group Pnma, in which though all the Sr^{2+} ions can be divided into two different types with the SrO_9 polyhedron, both Sr^{2+}

sites have the same symmetry (C_s) with slightly different site sizes [12,16,28,29]. Different from Ce^{3+} with f-d transitions [12], the 4f-4f transitions of Dy^{3+} ion are forbidden transitions, which are not affected mostly by the host structure. When Dy^{3+} ions located in slightly different Sr^{2+} sites, there should be no obvious change about the spectroscopic properties including fluorescence intensity and location of the excitation and emission peaks in ultraviolet (UV) – visible region. So the next spectral discussion is based on the Dy^{3+} in whole Sr^{2+} sites (Sr1+Sr2), not distinguishing between Dy^{3+} in Sr1 site and Dy^{3+} in Sr2 site.

Fig. 2 and Fig. 3 show the emission spectra of phosphors α-$Sr_{2(1-x)}Dy_{2x}P_2O_7$ and α-$Sr_{2(1-2x)}Dy_{2x}Li_{2x}P_2O_7$ with different x values upon 350 nm excitation, respectively. The two series of phosphors present similar spectral characteristic in shape, that is, the emission spectra consist of two dominating peaks around 478 nm and 574 nm, corresponding to $^4F_{9/2}\rightarrow{}^6H_{15/2}$ and $^4F_{9/2}\rightarrow{}^6H_{13/2}$ transitions of Dy^{3+}, respectively [4]. Meanwhile, the two series of phosphors also present different emission intensity, which is obviously due to the different doping concentrations of Dy^{3+} and Dy^{3+}/Li^+ in α-$Sr_2P_2O_7$ host. In order to show more clearly the variation trend of emission intensity with doping concentration (x), we plot the intensity (I) vs. dopant (x) curves for the two series of phosphors α-$Sr_{2(1-x)}Dy_{2x}P_2O_7$ and α-$Sr_{2(1-2x)}Dy_{2x}Li_{2x}P_2O_7$ in Fig. 4(a) and 4(b), respectively (λ_{ex} = 350 nm, λ_{em} = 574 nm). Interestingly, two obvious phenomenons can be observed. First, though so-called concentration quenching phenomenon is observed in above two series of phosphors, the optimal doping concentration of Dy^{3+} is different (0.005 for α-$Sr_{2(1-x)}Dy_{2x}P_2O_7$ and 0.03 for

α-$Sr_{2(1-2x)}Dy_{2x}Li_{2x}P_2O_7$). Second, the emission intensity of phosphors α-$Sr_{2(1-2x)}Dy_{2x}Li_{2x}P_2O_7$ far exceed that of phosphors α-$Sr_{2(1-x)}Dy_{2x}P_2O_7$ with the same x value. A typical example (x = 0.03), the emission intensity of α-$Sr_2P_2O_7$:Dy^{3+},Li^+ is about 8 times of that of α-$Sr_2P_2O_7$:Dy^{3+}. This obvious improvement of emission intensity and augment of optimal concentration of Dy^{3+} with Li^+ codoping can be attributed to the charge compensation phenomenon [5].

The concentration quenching phenomenon of the active ions is often due to the energy transfer (ET) from one activator to another until all the energy is consumed. From the above concentration quenching data, we can obtain an important parameter R_c, which is the critical distance where the probability of the nonradiative transfer is equal to the probability of the radiative emission [30]. So the value of R_c can be estimated from the following formula:

$$R_c = 2\left(\frac{3V}{4\pi x_c N}\right)^{1/3} \quad (1)$$

Where V is the volume of the unit cell, x_c is the critical concentration of activator ion, and N is the number of formula units per unit cell. According to the crystal structure of the α-$Sr_2P_2O_7$ compound [29], V = 639.79(3) $Å^3$, N = 4. The x_c have two values 0.005 for α-$Sr_{2(1-x)}Dy_{2x}P_2O_7$ and 0.03 for α-$Sr_{2(1-2x)}Dy_{2x}Li_{2x}P_2O_7$. Therefore, R_c was reckoned to be 39.4 Å and 21.6 Å for α-$Sr_{2(1-x)}Dy_{2x}P_2O_7$ and α-$Sr_{2(1-2x)}Dy_{2x}Li_{2x}P_2O_7$, respectively.

Generally speaking, the concentration quenching mechanism of active ions can be understood by Dexter theory, in which a link between the emission intensity (I) and activator concentration (x) was suggested at a given host lattice [31]. The emission

intensity (I) per activator ion concentration (x) can be expressed by the following equation:

$$\frac{I}{x} = \frac{k}{1+\beta(x)^{\theta/3}} \quad (2)$$

where k and β are constants for each interaction for a given host lattice; θ = 6, 8, 10 for dipole-dipole (d-d), dipole-quadrupole (d-q), quadrupole-quadrupole (q-q) interactions, respectively. The above equation can be rearranged further for $\beta(x)^{\theta/3} \gg 1$ as follows:

$$\lg(\frac{I}{x}) = K' - \frac{\theta}{3}\lg(x) \quad (3)$$

Where $K' = \lg K - \lg\beta$. So, the θ value can be obtained in term of the above equation. As the critical concentration of Dy^{3+} has been determined as 0.03 for α-$Sr_{2(1-2x)}Dy_{2x}Li_{2x}P_2O_7$ phosphors, the dependence of the emission intensity of the α-$Sr_{2(1-2x)}Dy_{2x}Li_{2x}P_2O_7$ phosphors excited at 350 nm on the Dy^{3+} concentration which is not less than the critical concentration (0.03) is determined, as shown in Fig. 5(a). The dependence of lg(I/*x*) on lg(*x*) is found to be relatively linear and the slope (-θ/3) is determined to be -1.83. Then the value of θ could be calculated as 5.52, which is approximatively equal to 6. Thus, the above result indicates that d-d interaction is key mechanism for the concentration quenching of Dy^{3+} emission in the α-$Sr_{2(1-2x)}Dy_{2x}Li_{2x}P_2O_7$ phosphors. However, by using the above same method, the slope (-θ/3) value obtained is -1.36 for Dy^{3+} emission in α-$Sr_{2(1-x)}Dy_{2x}P_2O_7$ phosphors in Fig. 5(b). The θ value is about 4.08, and far different from the value (6) indicating the d-d interaction. In many Dy^{3+} doped phosphors (e.g. $Ca_3Y_2(Si_3O_9)_2:Dy^{3+}$ [4],

Sr_2CeO_4:Dy^{3+} [5], , $Ba_3Y(PO_4)_3$:Dy^{3+} [6], $CaWO_4$:Dy^{3+} [9], $NaSrPO_4$:Dy^{3+} [32], etc.), the d-d interaction is proved to play an important role on the quenching of emission intensity of Dy^{3+} ions, so we think the d-d interaction among Dy^{3+} ions is the nature of concentration quenching phenomenon of Dy^{3+} emission in phosphor without other interaction type. In our cases, the interaction mechanism is not obviously d-d interaction for Dy^{3+} emission in α-$Sr_{2(1-x)}Dy_{2x}P_2O_7$ phosphors, indicating other interaction type (e.g. energy transfer) take effect [5]. Obviously, the concentration quenching mechanism of Dy^{3+} ions in α-$Sr_2P_2O_7$ with Li^+ charge compensation and without Li^+ charge compensation is different.

As we known, the $^4F_{9/2}\rightarrow{}^6H_{13/2}$ transition of Dy^{3+} ion belongs to the hypersensitive transition with $\Delta J = 2$, which is strongly influenced by the local environment of Dy^{3+} in a defined host, and is prominent when Dy^{3+} ions are located at low-symmetry sites without inversion centers according to the parity selection rule. So the Dy^{3+} site can be lowly symmetric with no inversion centers, because the emission intensity of $^4F_{9/2}\rightarrow{}^6H_{13/2}$ transition is more than that of $^4F_{9/2}\rightarrow{}^6H_{15/2}$ transition [4,7], as shown in Fig. 2 and Fig. 3. The above results are also coincident with the crystal structure of α-$Sr_2P_2O_7$, in which Sr^{2+} sites have C_s symmetry in α-$Sr_2P_2O_7$ host lattice [12,16,28]. Furthermore, the relative intensity ratio (Y/B) of yellow light ($^4F_{9/2}\rightarrow{}^6H_{13/2}$) to blue light ($^4F_{9/2}\rightarrow{}^6H_{15/2}$) can be adopted as sensitive parameter for understanding the structural distortion around Dy^{3+} ions in the α-$Sr_2P_2O_7$ host [4,7]. The value of Y/B shows a slight increasing trend with the increase of Dy^{3+} contents in α-$Sr_{2(1-x)}Dy_{2x}P_2O_7$ and α-$Sr_{2(1-2x)}Dy_{2x}Li_{2x}P_2O_7$, as shown in Fig. 6(a) and 6(b),

revealing that the local structural symmetry around Dy^{3+} ions decreases with the increase of Dy^{3+} contents, which is consistent with other Dy^{3+}-doped luminescent materials [33,34]. Meanwhile, the Y/B ratio shows negligible difference between α-$Sr_{2(1-x)}Dy_{2x}P_2O_7$ and α-$Sr_{2(1-2x)}Dy_{2x}Li_{2x}P_2O_7$ phosphors at a definite x value , indicating the effect of Li^+ on the local structural symmetry around Dy^{3+} ions with is infinitesimal.

The decay curves (λ_{ex} = 350 nm, λ_{em} = 574 nm) of the as-prepared phosphors α-$Sr_{2(1-x)}Dy_{2x}P_2O_7$ and α-$Sr_{2(1-2x)}Dy_{2x}Li_{2x}P_2O_7$ with different Dy^{3+} contents (x value) were also measured. As two typical examples, Fig. 7(a) and 7(b) show the decay curves with x = 0.03, because all curves exhibit the single exponential decay behavior. The lifetimes (τ) were calculated for all samples in term of a single exponential equation

$$I_t = I_0 \exp(-t/\tau) \quad (4)$$

where I_t and I_0 are intensities at time t and zero time, and τ is the fluorescence lifetime for the exponential components, as shown in Fig. 7(e) for α-$Sr_{2(1-2x)}Dy_{2x}Li_{2x}P_2O_7$ and Fig. 7(f) for α-$Sr_{2(1-x)}Dy_{2x}P_2O_7$, respectively. The lifetime seems to keep constant (~1.05 ms) for α-$Sr_{2(1-x)}Dy_{2x}P_2O_7$ phosphors, and show decreasing tendency (from 0.99 ms to 0.914 ms) for α-$Sr_{2(1-2x)}Dy_{2x}Li_{2x}P_2O_7$ with the increase of Dy^{3+} contents. Moreover, at a definite Dy^{3+} content, Li^+ charge compensating sample α-$Sr_2P_2O_7$:Dy^{3+},Li^+ shows more quicker decay behavior than that of no Li^+ compensation sample α-$Sr_2P_2O_7$:Dy^{3+}.

According to the above experimental results, we can find that Li^+ ion has important

effect on the luminescence properties of α-$Sr_2P_2O_7$:Dy^{3+} including emission intensity, optimal doping concentration, concentration quenching mechanism, and fluorescence lifetime, which was discussed in detail as follows. In our samples, there are two series of phosphors: no charge compensating α-$Sr_2P_2O_7$:Dy^{3+} and Li^+-compensating α-$Sr_2P_2O_7$:Dy^{3+},Li^+. As to the former, equivalent mole substitution of divalent Sr^{2+} ions by trivalent Dy^{3+} ions must lead to the defects generation in as-prepared phosphors in order to keep charge balance, because there are not other phases in view of the XRD results in Fig. 1, and these defects can be with negative charge. Thus, some possible cases should be considered. (1) Three Sr^{2+} ions would be substituted by two Dy^{3+} ions and consequently a Sr^{2+} vacancy (V''_{Sr}) would also be created according to the possible process $3Sr_{Sr} \rightarrow 2Dy_{Sr}^{\bullet} + V''_{Sr}$. These Sr^{2+} vacancies can act as defect sites and reduce the overall luminescence intensity due to the energy transfer from luminescence centers to the vacancy defects [22]. Meanwhile, some extra Dy^{3+} ions do not enter into the lattice site properly, and exist in oxides (Dy_2O_3) with minute quantity. The above condition can be possible because a very small amount of oxides would be not detected in the XRD measurement. (2) Two Sr^{2+} ions would be substituted by two Dy^{3+} ions and consequently an interstitial O_i'' defect in the vicinity of the $Dy_{Sr}^{\bullet}$ would be created according to the possible process $2Sr_{Sr} \rightarrow 2Dy_{Sr}^{\bullet} + O_i''$. These interstitial O_i'' defects act as killers of luminescence and energy migration through them quenches the luminescence. The above condition can be also possible because when the sample is sintered in air, the ambient oxygen can penetrate into the permeable crystal structure [35]. (3) Two Sr^{2+} ions would be substituted by

two Dy^{3+} ions and consequently an oxygen vacancy V_O'' would be created according to the possible process $2Sr_{Sr} \rightarrow 2Dy_{Sr}^{\bullet} + V_O''$. The V_O'' can also lead to the decrease of luminescence intensity. However, the oxygen vacancies often appear in the phosphor prepared in a reducing atmosphere [8]. As our samples were prepared in air, the oxygen vacancies can not be primary defect type appearing in α-$Sr_2P_2O_7$:Dy^{3+}, in which V''_{Sr} and/or O_i'' could exist as chief defect types to take effect on the luminescence properties of Dy^{3+} ions. As to α-$Sr_2P_2O_7$:Dy^{3+},Li^+, two Sr^{2+} ions would be substituted by a Dy^{3+} ion and a Li^+ ion according to the possible process $2Sr_{Sr} \rightarrow Dy_{Sr}^{\bullet} + Li_{Sr}'$, and no defects can be produced in theory. As the defects (V''_{Sr}, O_i'', and V_O'') can trap the electrons from the excited levels of Dy^{3+} ion and quench the luminescence of α-$Sr_2P_2O_7$:Dy^{3+}, the weaker emission intensity can be obtained in α-$Sr_2P_2O_7$:Dy^{3+} relative to that of α-$Sr_2P_2O_7$:Dy^{3+},Li^+ (see Fig. 4). In addition, we also can not ignore that Li_2CO_3 may act as the role of solid flux in the experiment, and stimulate the host lattice formation and grain growth, leading to higher oscillator strengths for the optical transitions [23]. Fig. 8(a) and 8(b) show the SEM and size distribution images of α-$Sr_{2(1-x)}Dy_{2x}P_2O_7$ (x = 0.03) and α-$Sr_{2(1-2x)}Dy_{2x}Li_{2x}P_2O_7$ (x = 0.03), respectively. Obviously, the size and agglomeration of particles for Li^+-containing sample is much larger than that for no Li^+-containing sample due to the effect of Li_2CO_3 as solid flux. So, the emission intensity of phosphors α-$Sr_{2(1-2x)}Dy_{2x}Li_{2x}P_2O_7$ far exceed that of phosphors α-$Sr_{2(1-x)}Dy_{2x}P_2O_7$ with the same x value based on the above analysis. Furthermore, concentration quenching phenomenon of Dy^{3+} in many phosphors can be explained in term of cross relaxation

processs (e.g. via the $^4F_{9/2} \rightarrow {}^6H_{9/2}$ + $^6F_{11/2}$ and $^6H_{15/2} \rightarrow {}^6F_{3/2}$ transitions) [9,36], which become more efficient with more Dy^{3+} doping. But in α-$Sr_2P_2O_7$:Dy^{3+}, more defects (quenching sites) can be produced with the increase of Dy^{3+} contents, which can quench the fluorescence intensity of Dy^{3+} in α-$Sr_2P_2O_7$:Dy^{3+} with greater magnitude. That is the main reason that optimal doping concentration of Dy^{3+} in α-$Sr_2P_2O_7$:Dy^{3+} (0.005) is much lower than that in α-$Sr_2P_2O_7$:Dy^{3+},Li^+ (0.03) (see Fig. 4). In fact, the role of solid flux for Li_2CO_3 can also enlarge the optimal doping concentration of Dy^{3+} in phosphors to some content. As the efficient energy transfer from Dy^{3+} to defects in α-$Sr_2P_2O_7$:Dy^{3+}, the concentration quenching mechanism spontaneously deviate from d-d interaction as the nature concentration quenching phenomenon of Dy^{3+} emission in phosphor without other interaction type. Different variation tendency of decay time with Dy^{3+} contents also illustrate the effect of defects in phosphors α-$Sr_2P_2O_7$:Dy^{3+} and α-$Sr_2P_2O_7$:Dy^{3+},Li^+. Usually, the decay time of the transition from $^4F_{9/2}$ to lower energy level (e.g. $^6H_{13/2}$) shows the decreasing tendency with the increase of Dy^{3+} contents, which may be due to the more efficient energy transfer process among Dy^{3+} ions (cross relaxation process) at higher Dy^{3+} concentrations [8,34,36]. Similar variation tendency was found in our samples α-$Sr_2P_2O_7$:Dy^{3+},Li^+ (see Fig. 7). As there are some defects in α-$Sr_2P_2O_7$:Dy^{3+} as discussed above, these defects could play a "pulling electron" role that the energy transfer process from the excited energy level to defects could inhibit the radiative transition process of Dy^{3+} from $^4F_{9/2}$ to $^6H_{13/2}$ to some extent, which leads to the much slower decay behavior in α-$Sr_2P_2O_7$:Dy^{3+} than that in α-$Sr_2P_2O_7$:Dy^{3+},Li^+. With the

increase of Dy^{3+} contents in α-$Sr_2P_2O_7$:Dy^{3+}, the inhibiting role became more efficient so that the decay time for the transition $^4F_{9/2}\rightarrow{}^6H_{13/2}$ in α-$Sr_2P_2O_7$:Dy^{3+} seems to be not significantly different.

As the sample α-$Sr_{2(1-2x)}Dy_{2x}Li_{2x}P_2O_7$ (x = 0.03) shows the much stronger emission intensity than that in other samples, its excitation spectrum recorded in the spectral range of 250–550 nm is plotted in Fig. 9 by monitoring the emission at 574 nm corresponding to the $^4F_{9/2}\rightarrow{}^6H_{13/2}$ transition of Dy^{3+}. A series of line-shaped excitation peaks peaking at 299 nm, 325 nm, 350 nm, 364 nm, 386 nm, 426 nm, 448 nm, 473 nm can be observed in the curve (a), which can correspond with the electronic transitions from the ground state $^6H_{15/2}$ to the excited states $^4K_{13/2}$, $^4K_{15/2}$, $^4M_{15/2}$+$^6P_{7/2}$, $^4I_{11/2}$, $^4I_{13/2}$+ $^4F_{7/2}$, $^4G_{11/2}$, $^4I_{15/2}$, $^4F_{9/2}$ of Dy^{3+} in $Sr_2P_2O_7$ host, respectively [34,37]. Among all the excitation peaks, the peak at 350 nm possesses the maximum intensity, which is coincident with that in many Dy^{3+} doped phosphors. Some possible broad excitation bands including the $O^{2-}\rightarrow Dy^{3+}$ charge-transfer band and $4f^9$-$4f^8$5d excitation band of Dy^{3+} as well as the host-related absorption band are not observed in the UV wavelength range owing to their higher energy below 200 nm [3,12,38]. The above excitation bands locating in the wavelength 300–400 nm matches partly with the emitting of NUV chips, indicating the potential application for NUV w-LEDs [8,37].

The CIE color coordinates and color correlated temperature (CCT) are the important parameters for evaluating white-light-emitting phosphors' performance. Thus, as a case, the CIE chromaticity coordinates of the sample α-$Sr_{2(1-2x)}Dy_{2x}Li_{2x}P_2O_7$ (x = 0.03)

is calculated to be (0.339, 0.39) and shown in Fig. 10, which is located in the white region. The value of CCT is also calculated to be about 5313 K in term of the method given by McCamy [9,39], which is close to that (~5500 K) of sunlight at noon.

4. Conclusions

Two series of phosphors α-$Sr_{2(1-x)}Dy_{2x}P_2O_7$ and α-$Sr_{2(1-2x)}Dy_{2x}Li_{2x}P_2O_7$ with different x values were synthesized successfully using a solid state method at 1173 K. The comparative luminescence properties of the Dy^{3+} doped and Dy^{3+}-Li^+ co-doped α-$Sr_2P_2O_7$ phosphors have been carefully investigated for the first time. Some results can be found as follows. (1) Li^+ ion co-doping leads to the luminescent enhancement of Dy^{3+} in α-$Sr_2P_2O_7$ host lattice; (2) The optimal doping concentration of Dy^{3+} in α-$Sr_2P_2O_7$:Dy^{3+},Li^+ is much larger than that in α-$Sr_2P_2O_7$:Dy^{3+}; (3) The concentration quenching mechanism of Dy^{3+} emission in α-$Sr_2P_2O_7$:Dy^{3+} deviates from that in α-$Sr_2P_2O_7$:Dy^{3+},Li^+ (d-d interaction); (4) The $^4F_{9/2}\rightarrow{}^6H_{13/2}$ transition of Dy^{3+} in α-$Sr_2P_2O_7$:Dy^{3+} shows much slower decay behavior than that in α-$Sr_2P_2O_7$:Dy^{3+},Li^+. The effect of Dy^{3+} ion on the luminescence properties of phosphors was mainly discussed in term of the defect generation in α-$Sr_2P_2O_7$:Dy^{3+} as well as the charge compensation and effect of solid flux expected in phosphors with Li^+ co-doping in detail. White light emission can obtained in the as-prepared phosphors upon UV light excitation, in which the CIE chromaticity coordinates and color correlated temperature were calculated to be (0.339, 0.39) and 5313 K for the phosphor α-$Sr_{2(1-2x)}Dy_{2x}Li_{2x}P_2O_7$ (x = 0.03) with the optimal fluorescence intensity, respectively. The present work could not only enlarge the scope of research on luminescence

properties of α-$Sr_2P_2O_7$ based phosphor, but provided some idea on the development of novel white light emitting phosphors through non-equivalent displacement by efficiently taking advantage of charge compensator (e.g. Li^+ ion) for potential application in solid state lighting (e.g. w-LEDs).

Acknowledgments

The work is financially supported by the National Natural Science Foundation of China (no. 21271111), the Science and Technology Project of Henan Province (no. 142300410245), and the Doctoral Scientific Research Foundation of Zhengzhou University of Light Industry (no. 2013BSJJ001).

References

[1] M. M. Shang, C. X. Li and J. Lin, *Chem. Soc. Rev.*, 2014, 43, 1372−1386.

[2] H. A. Höppe, *Angew. Chem. Int. Ed.*, 2009, 48, 3572−3582.

[3] J. P. Zhong, H. B. Liang, B. Han, Z. F. Tian, Q. Su and Y. Tao, *Opt. Express*, 2008. 16, 7508−7515.

[4] Z. P. Yang, H. Y. Dong, X. S. Liang, C. C. Hou, L. P. Liu and F. C. Lu, *Dalton Trans.*, 2014, 43, 11474–11477.

[5] D. L. Monika, H. Nagabhushana, R. Hari Krishna, B. M. Nagabhushana, S. C. Sharma and T. Thomas, RSC Adv., 2014, 4, 38655–38662.

[6] Q. B. Liu, Y. F. Liu, Y. J. Ding, Z. M. Peng, X. D. Tian, Q. M. Yu and G. Y. Dong, *Ceram. Int.*, 2014, l40, 10125–10129.

[7] M. H. Tong, Y. J. Liang, G. G. Li, Z. G. Xia, M. F. Zhang, F. Yang and Q. Wang, *Opt. Mater.*, 2014, 36, 1566–1570.

[8] Z. P. Ci, Q. S. Sun, S. C. Qin, M. X. Sun, X. J. Jiang, X. D. Zhang and Y. H. Wang, *Phys. Chem. Chem. Phys.*, 2014, 16, 11597–11602.

[9] A. K. Ambast, J. Goutam, S. Som and S. K. Sharma, *Spect. Acta Part A*, 2014, 122, 93–99.

[10] G. Zhu, Y. H. Wang, Q. Wang, X. Ding, W. Y. Geng and Y. R. Shi, *J. Lumin.*, 2014, 154, 246–250.

[11] X. M. Zhang, W. Jiang, Q. Pan, G. M. Yuan and H. J. Seo, *Mater. Lett.*, 2014, 128, 89–92.

[12] D. J. Hou, B. Han, W. P. Chen, H. B. Liang, Q. Su, P. Dorenbos, Y. Huang, Z. H. Gao and Y. Tao, *J. Appl. Phys.*, 2010, 108, 083527.

[13] M. Mohapatra, A. K. Yadav, S. N. Jha, D. Bhattacharyya, S. V. Godbole and V. Natarajan, *Chem. Phys. Lett.*, 2014, 601, 81–86.

[14] M. Y. Peng and L. Wondraczek, *Opt. Lett.*, 2010, 35, 2544–2546.

[15] S. Ye, Z. S. Liu, J. G. Wang and X. P. Jing, *Mater. Res. Bull.*, 2008, 43, 1057–1065.

[16] D. J. Hou, C. M. Liu, X. J. Kuang and H. B. Liang, *Opt. Express*, 2012, 20, 28969–28980.

[17] L. X. Wang, M. J. Xu, R. Sheng, L. Liu and D. Z Jia, *J. Alloys Compd*., 2013, 579, 343–347.

[18] M. J. Xu, L. X. Wang, L. Liu, D. Z. Jia and R. Sheng, *J. Lumin.*, 2014, 146, 475–479.

[19] R. Pang, C. Y. Li, L. L. Shi and Qiang Su, *J. Phys. Chem. Solids*, 2009, 70,

303–306.

[20] G. F. Ju, Y. H. Hu, L. Chen, X. J. Wang and Z. F. Mu, *Mater. Res. Bull.*, 2013, 48, 4743–4748.

[21] N. Patel, M. Srinivas, V. Vishwnath, D. Modi and K. V. R. Murthy, Int. J. ChemTech Res. 2014, 6, 1708–1711.

[22] S. Saha, S. Das, U. K. Ghorai, N. Mazumder, B. K. Gupta and K. K. Chattopadhyay, *Dalton Trans.*, 2013, 42, 12965–12974.

[23] Y. B. Wu, Z. Sun, K. B. Ruan, Y. Xu and H. Zhang, *J. Lumin.*, 2014, 155, 269–274.

[24] R. P. Cao, G. Chen, X. G. Yu, C. Y. Cao, K. B. Chen, P. Liu and S. H. Jiang, *J. Solid State Chem.*, 2014, 220, 97–101.

[25] P. L. Li, Z. J. Wang, Z. P. Yang and Q. L. Guo, *J. Solid State Chem.*, 2014, 220, 227–231.

[26] Z. W. Zhang, Y. N. Wu, X. H. Shen, Y. Y. Ren, W. G. Zhang and D. J. Wang, *Opt. Laser Tech.*, 2014, 62, 63–68.

[27] B. Han, H. B. Liang, H. Y. Ni, Q. Su, G. T. Yang, J. Y. Shi and G. B. Zhang, *Opt. Express*, 2009, 17, 7138–7144.

[28] L. Hagman, I. Jansson, C. Magneli, O. Tolboe and J. Paasivirta, *Acta Chem. Scand.*, 1968, 22, 1419–1429.

[29] J. Barbier and J.-P. Echard, *Acta Cryst. C*, 1998, 54, IUC9800070.

[30] G. Blasse, *Philips Res. Repts.*, 1969, 24, 131–144.

[31] D. L. Dexter, *J. Chem. Phys.*, 1953, 21, 836–850.

[32] Z. F. Hu, T. Meng, W. Zhang, D. H. Ye, Y. P. Cui, L. Luo and Y. H. Wang, *J. Mater. Sci.: Mater. Electron.*, 2014, 25, 1933–1937.

[33] P. L. You, G. F. Yin, X. C. Chen, B. Yue, Z. B. Huang, X. M. Liao and Y. D. Yao, *Opt. Mater.*, 2011, 33, 1808–1812.

[34]T. Chengaiah, C. K. Jayasankar, K. Pavani, T. Sasikala and L. Rama Moorthy, *Opt. Commun.*, 2014, 312, 233–237.

[35] M. Y. Peng, J. C. Lei, L. Y. Li, L. Wondraczek, Q. Y. Zhang and J. R. Qiu, *J. Mater. Chem. C*, 2013, 1, 5303–5308.

[36] L. Marciniak, D. Hreniak and W. Strek, *J. Mater. Chem. C*, 2014, 2, 5704–5708.

[37] Z. W. Zhang, X. H. Shen, Y. S. Peng, Y. N. Wu, Z. Y. Mao, W. G. Zhang and D. J. Wang, *Mater. Lett.*, 2014, 117, 14–16.

[38] B. Han, H. B. Liang, H. H. Lin, W. P. Chen, Q. Su, G. T. Yang and G. B. Zhang, *J. Opt. Soc. Am. B*, 2008, 25, 2057–2063.

[39] C. S. McCamy, *Color Res. Appl.*, 1992, 17,142–144.

Captions of Figures

Fig. 1 The XRD patterns of the samples with x = 0.001, 0.005, 0.05 for α-$Sr_{2(1-x)}Dy_{2x}P_2O_7$ and x = 0.003, 0.03, 0.1 for α-$Sr_{2(1-2x)}Dy_{2x}Li_{2x}P_2O_7$ as well as the α-$Sr_2P_2O_7$ host.

Fig. 2 The emission spectra of phosphors α-$Sr_{2(1-x)}Dy_{2x}P_2O_7$ with different x values upon 350 nm excitation.

Fig. 3 The emission spectra of phosphors α-$Sr_{2(1-2x)}Dy_{2x}Li_{2x}P_2O_7$ with different x

values upon 350 nm excitation.

Fig. 4 The intensity (I) vs. dopant (x) curves for the two series of phosphors α-$Sr_{2(1-x)}Dy_{2x}P_2O_7$ and α-$Sr_{2(1-2x)}Dy_{2x}Li_{2x}P_2O_7$ (λ_{ex} = 350 nm, λ_{em} = 574 nm).

Fig. 5 Curves of lg(I/x) vs. lg(x) in α-$Sr_{2(1-x)}Dy_{2x}P_2O_7$ and α-$Sr_{2(1-2x)}Dy_{2x}Li_{2x}P_2O_7$ phosphors.

Fig. 6 Variation of the value of (Y/B) with the doping concentration of Dy^{3+} in α-$Sr_{2(1-x)}Dy_{2x}P_2O_7$ and α-$Sr_{2(1-2x)}Dy_{2x}Li_{2x}P_2O_7$ phosphors.

Fig. 7 The decay curves (left) of the as-prepared phosphors α-$Sr_{2(1-x)}Dy_{2x}P_2O_7$ and α-$Sr_{2(1-2x)}Dy_{2x}Li_{2x}P_2O_7$ with x = 0.03 and the variation of the lifetime (right) with the doping concentration of Dy^{3+} in α-$Sr_{2(1-x)}Dy_{2x}P_2O_7$ and α-$Sr_{2(1-2x)}Dy_{2x}Li_{2x}P_2O_7$ phosphors (λ_{ex} = 350 nm, λ_{em} = 574 nm).

Fig. 8 The SEM and size distribution images of α-$Sr_{2(1-x)}Dy_{2x}P_2O_7$ (x = 0.03) (a) and α-$Sr_{2(1-2x)}Dy_{2x}Li_{2x}P_2O_7$ (x = 0.03) (b).

Fig. 9 The excitation spectrum of α-$Sr_{2(1-2x)}Dy_{2x}Li_{2x}P_2O_7$ (x = 0.03) by monitoring the emission at 574 nm.

Fig. 10 The CIE chromaticity coordinates of α-$Sr_{2(1-2x)}Dy_{2x}Li_{2x}P_2O_7$ (x = 0.03) (λ_{ex} = 350 nm).

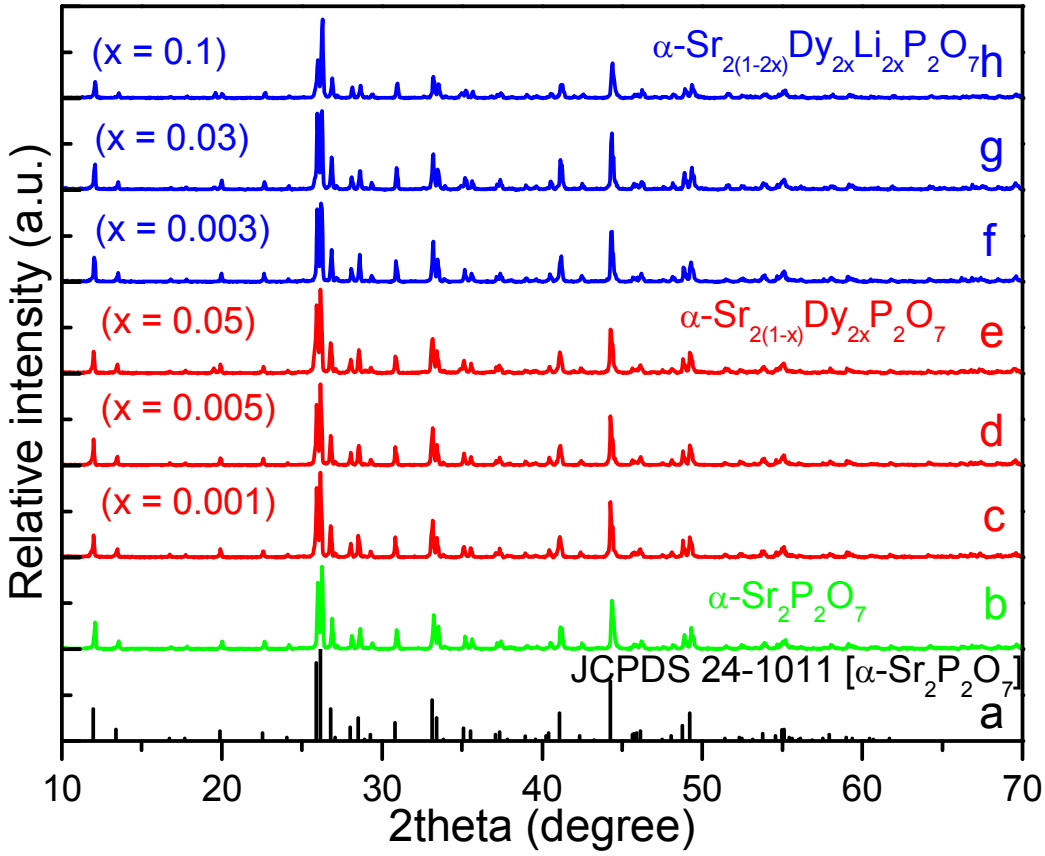

Fig. 1

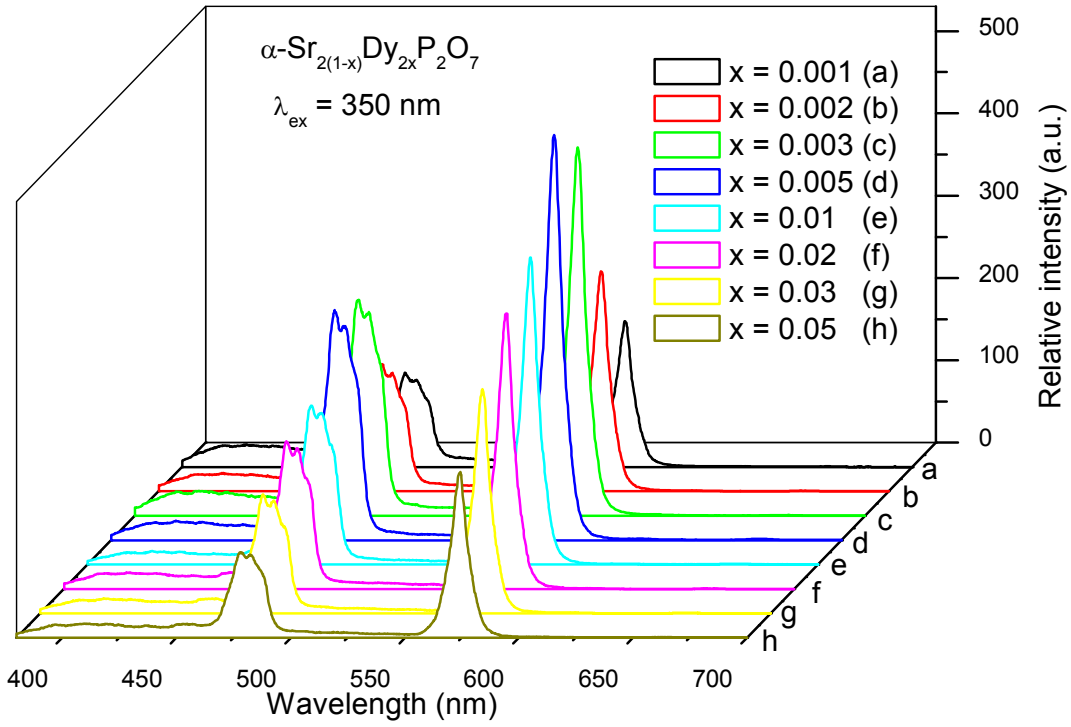

Fig. 2

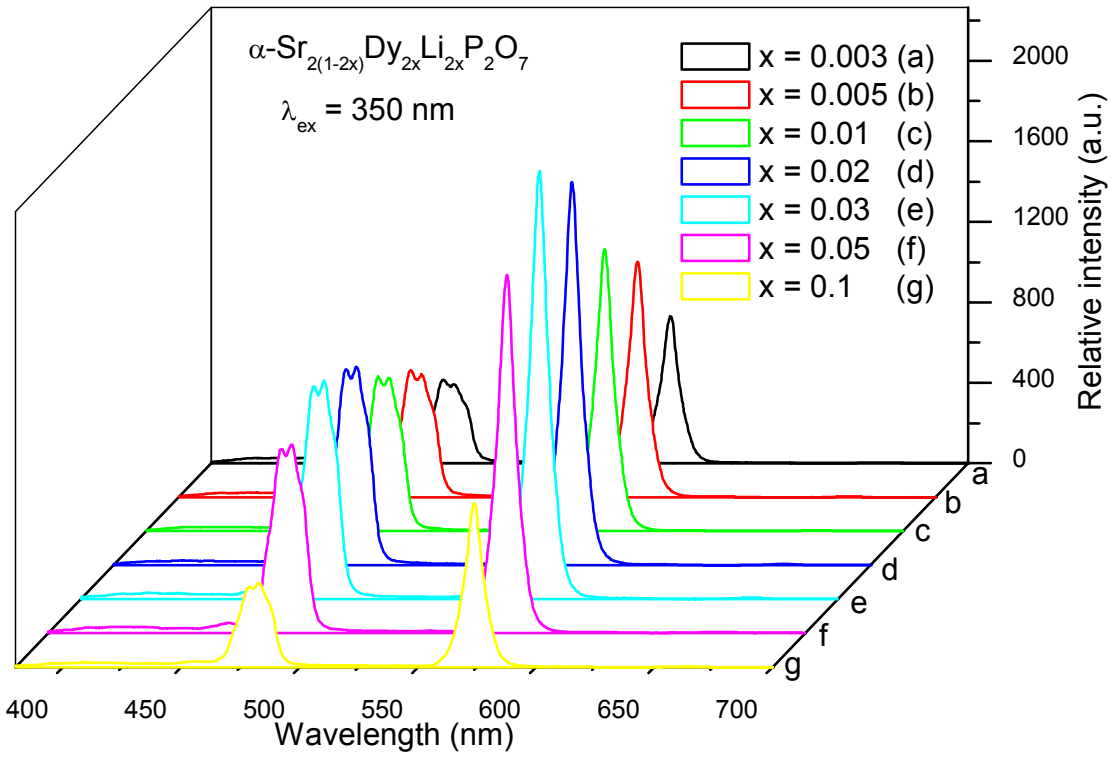

Fig. 3

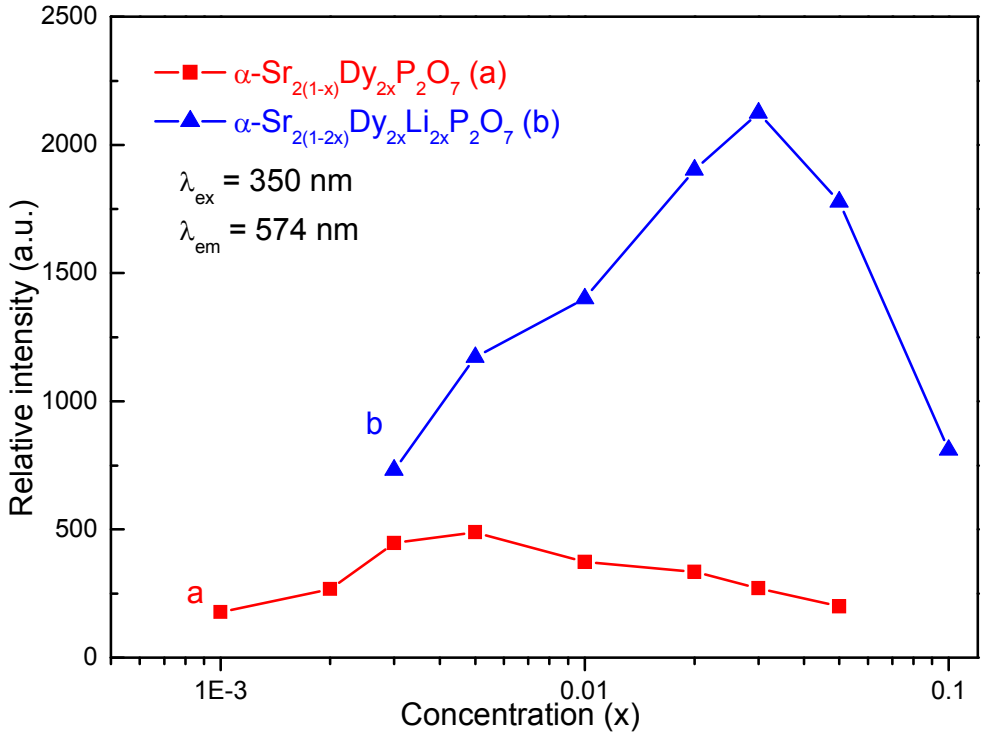

Fig. 4

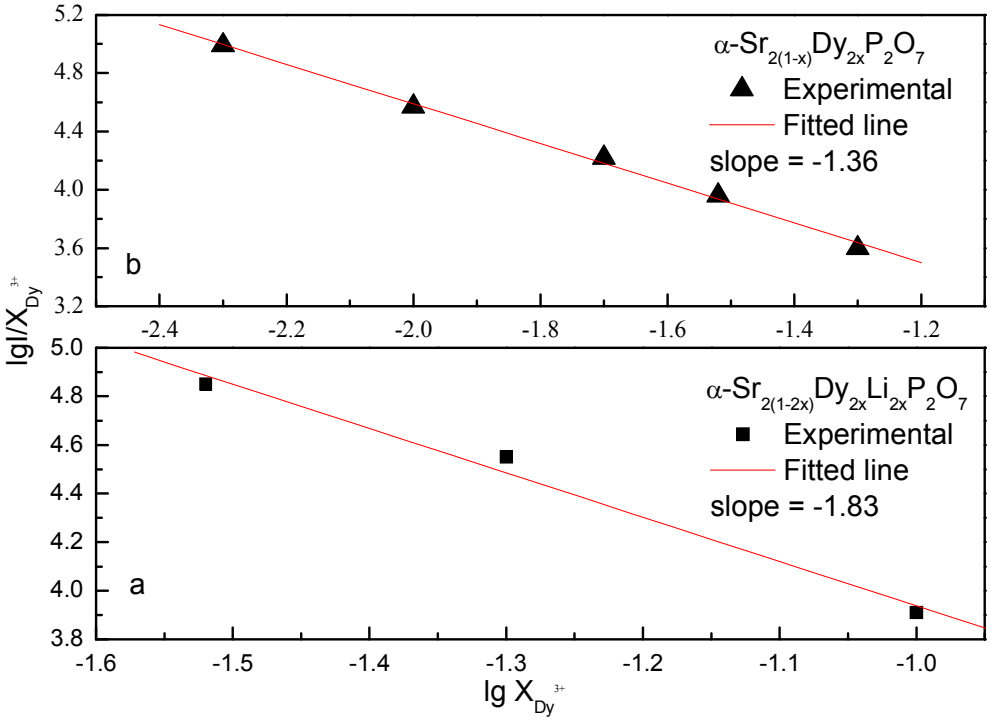

Fig. 5

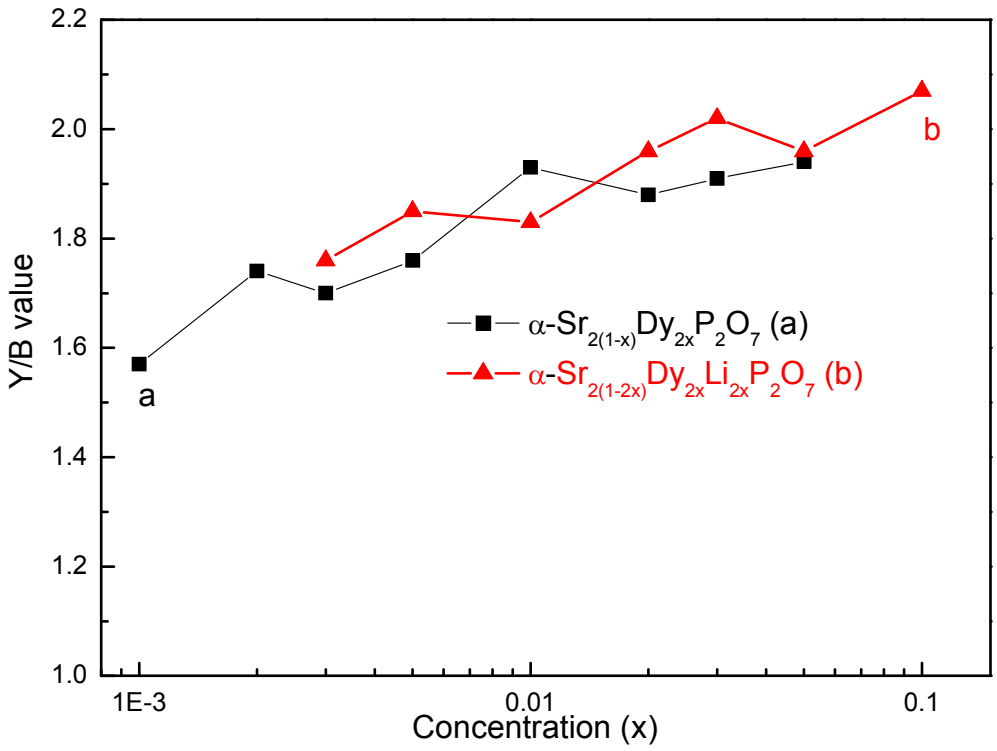

Fig. 6

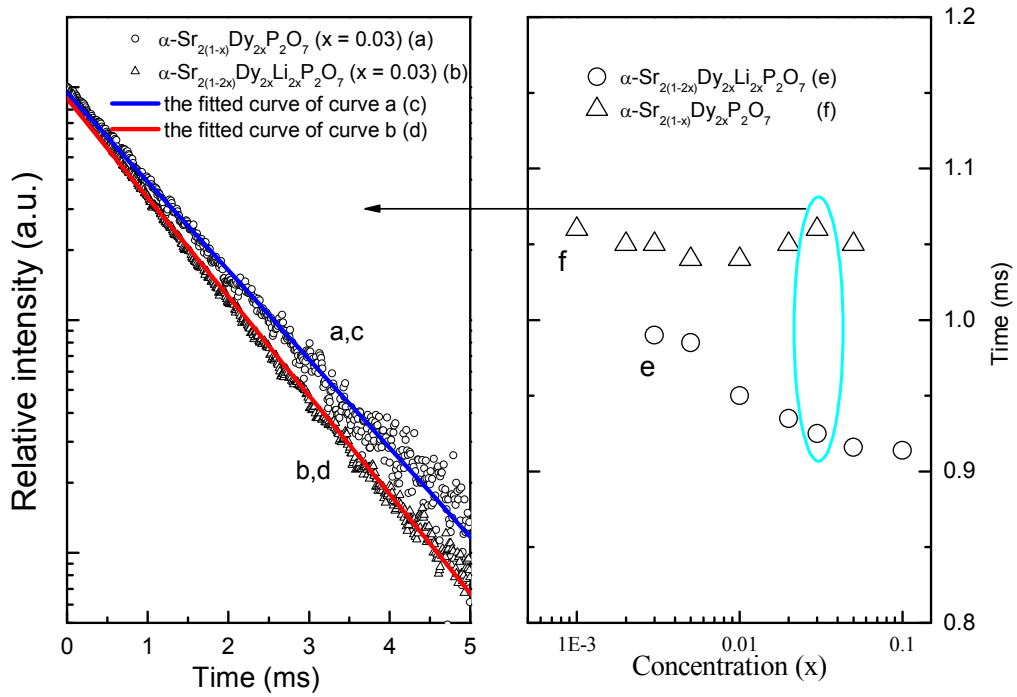

Fig. 7

]

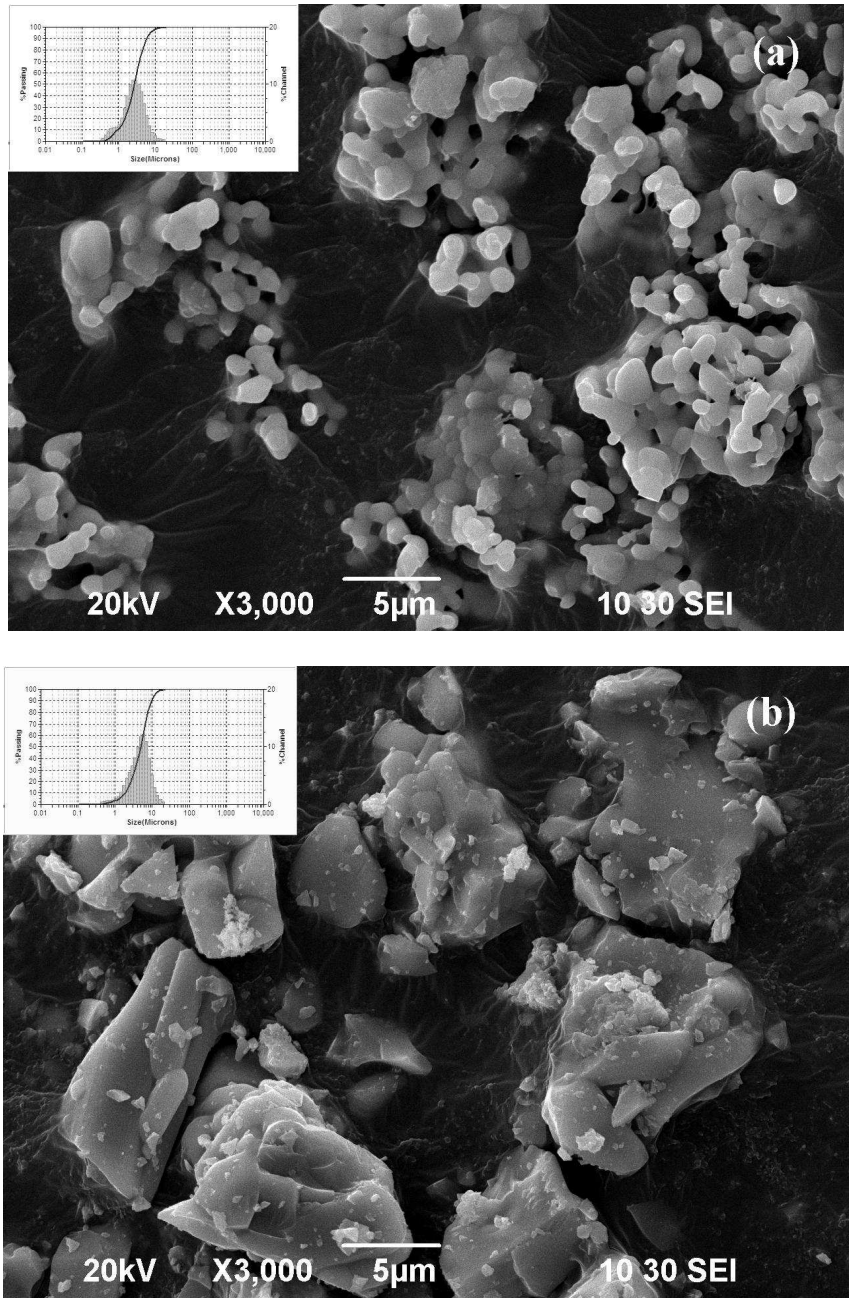

Fig. 8

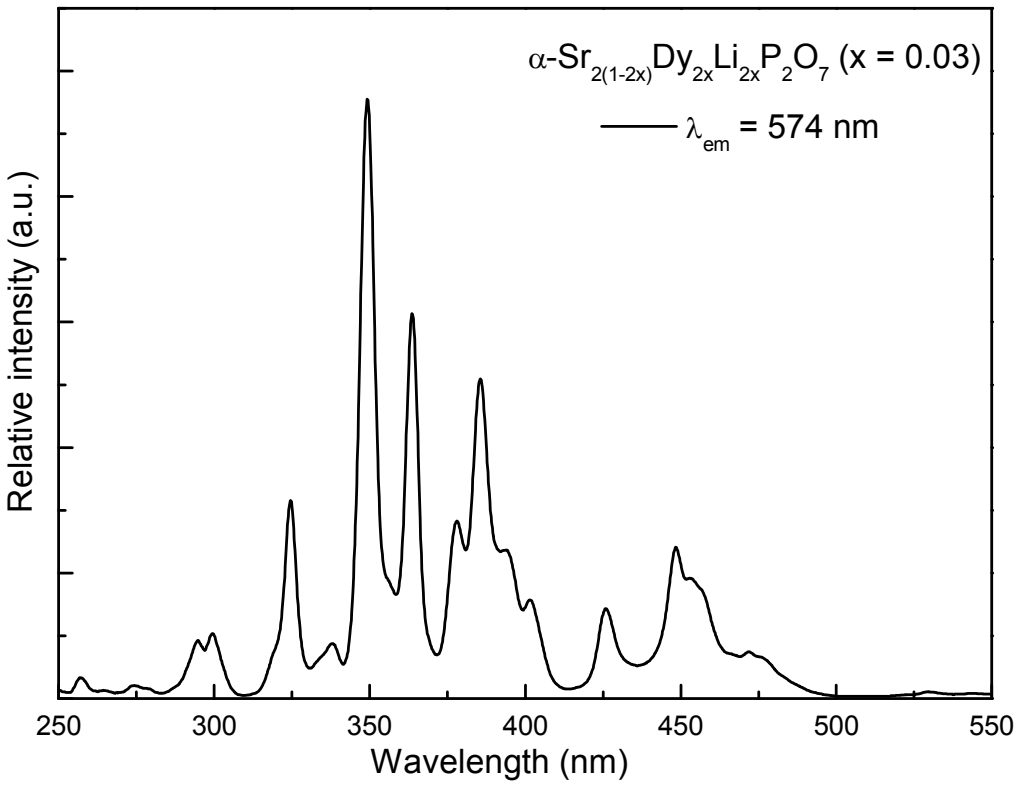

Fig. 9

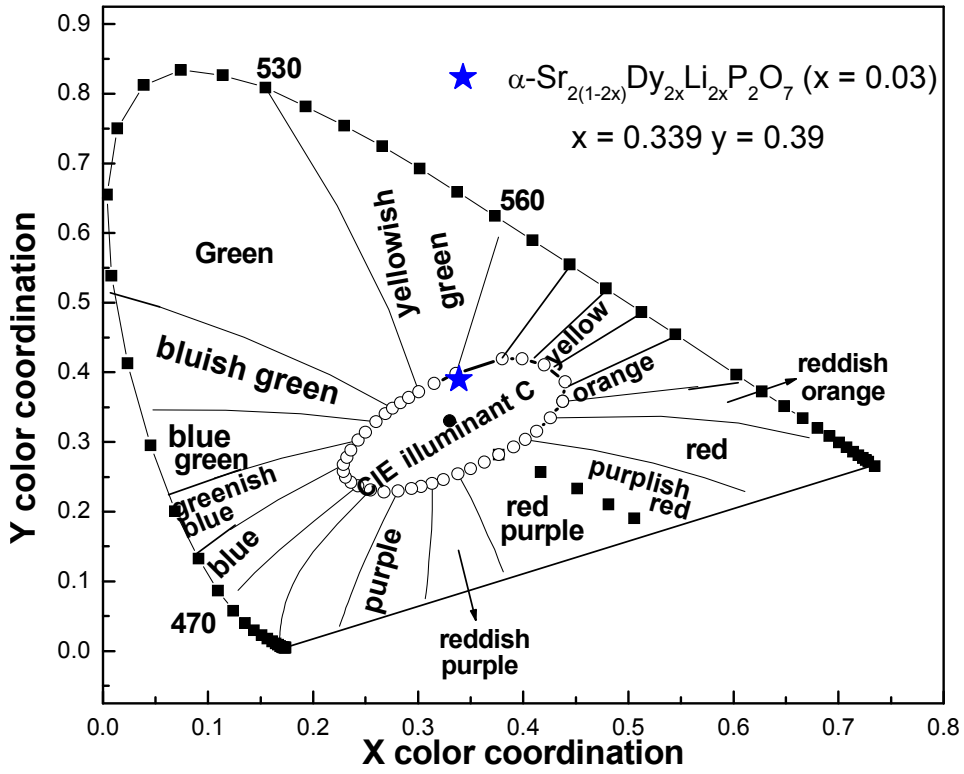

Fig. 10